

Carbon monoxide (CO), molecular nitrogen (N₂) and molecular oxygen (O₂) are predicted to be among the most abundant small molecules in dense cores. During the formation of these dense cores, the total oxygen and nitrogen budgets are expected to remain constant. However, the observed abundance of gas-phase oxygen is unexpectedly reduced by orders of magnitude from diffuse clouds ([O] = 3 × 10⁻⁴) to dense cores ([O₂] = 3-10 × 10⁻⁸)²⁻⁵. Moreover, although the observed abundance of gas-phase CO (≈10⁻⁴)⁶ is well reproduced by simulations, the models are unable to explain the formation and abundances of N₂ and O₂. The observed abundance of the latter is several orders of magnitude lower than predicted.^{4,7} To explain the apparent reduction of the oxygen budget during the collapse of a diffuse cloud and to help understand the discrepancies between observations and models, one has to consider processes taking place at the surface of the interstellar dust grains. These silicate grains are covered with an icy mantle at the low temperatures (≈ 10 K) encountered in the dense clouds, and the exchange between the solid and gas phases is crucial to determine molecular abundances. To this aim, we determined the kinetic parameters for the desorption of CO, N₂ and O₂ from bare silica by Temperature-Programmed Desorption (TPD) coupled with simulations.

The experiments are performed on the setup pictured on **Fig. 1**; it is composed of a central UHV chamber (base pressure 10⁻¹⁰ mbar) with a closed-cycle helium cryostat (base temperature ≈ 15 K) to mimic the grain temperatures encountered in the ISM. The sample, an oxygen free high conductivity copper block coated with amorphous silica, is mounted onto the end of a cold finger. The TPD experiments on background dosed O₂, CO and N₂ desorbing from the silica sample are realized with a heating ramp of 0.1 K.s⁻¹.

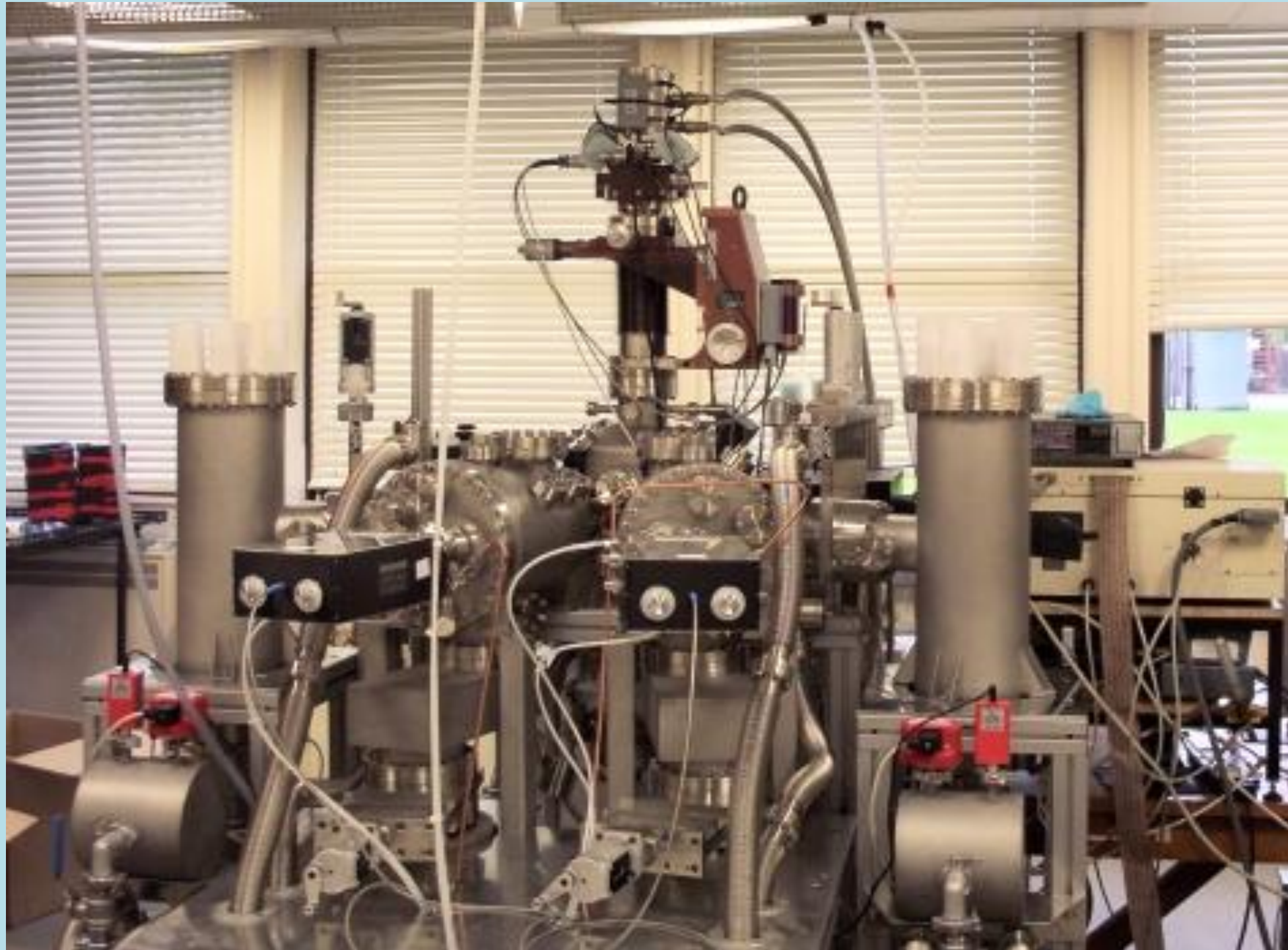


Figure 1: The experimental setup used for the TPD experiments.

Multilayers

Experimental TPD profiles (open circles on **Fig. 3**) exhibit roughly coincident leading edges. Plots of ln(*r*_{des}) vs. ln(*N*) (**Fig. 4**) show that CO and O₂ multilayers follow non-zero desorption order (cf. **Table 1**), contrary to the N₂ multilayer. The rough surface of the silica affects the desorption kinetics of the multilayers.

With the Chemical Kinetic Simulator⁸ software, fits of the TPD profiles (full lines on **Fig. 3**) → *v* and *E*_{des} are obtained for the desorption of CO, N₂ and O₂ multilayers from silica (cf. **Table 1**).

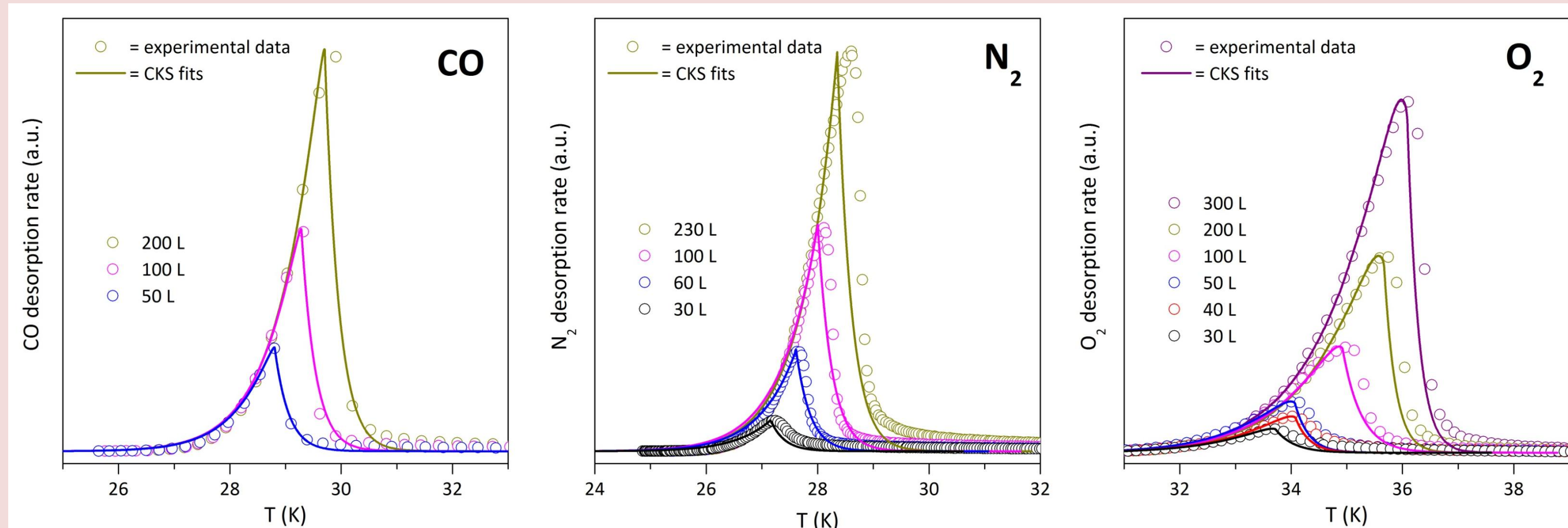


Figure 3: From left to right, TPD profiles (open circles) of CO, N₂ and O₂ multilayers desorbing from silica. The CKS fits are shown with full lines.

Species	<i>n</i>	<i>v</i> (molecules.cm ⁻²) ⁽¹⁻ⁿ⁾ .s ⁻¹	<i>E</i> _{des} (K)	<i>E</i> _{des} (K) from polycrystalline Au
CO	0.09 ± 0.11	10 ^{33±2}	1251 ± 240	854 ± 24 [9]
N ₂	0.00 ± 0.08	10 ^{34±2}	1179 ± 240	794 ± 24 [10]
O ₂	0.18 ± 0.04	10 ^{27±2}	1179 ± 240	914 ± 24 [9]

Table 1: Kinetic parameters for the desorption of CO, N₂ and O₂ multilayers from bare silica.

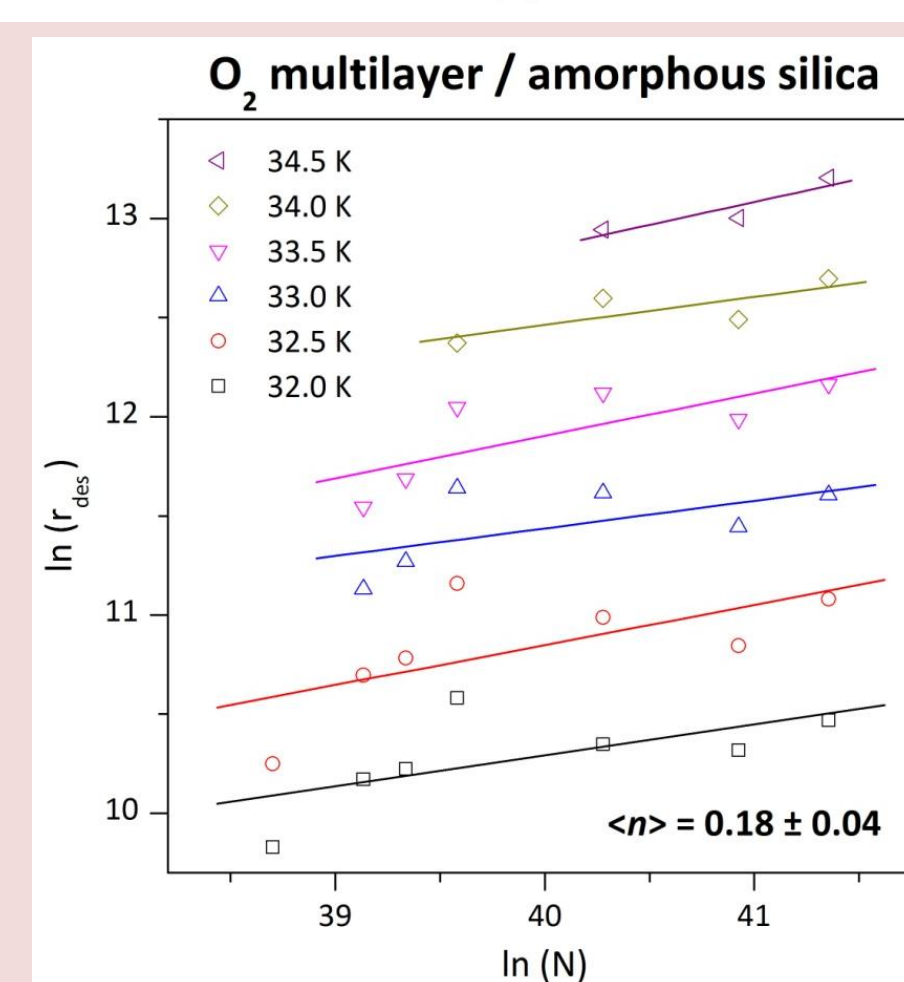


Figure 4: Plot of ln(*r*_{des}) as function of ln(*N*) for O₂. The average slope gives the desorption order *n*.

Our values of *v* and *E*_{des} are higher than in other studies, and outside of the error range for CO and N₂.¹¹

→ In these studies, assumption of *n* = 0 for the multilayer: could explain this difference.

→ Instability of our temperature calibration, which leads to an uncertainty in the measured *T* and to an overestimation of *v* and *E*_{des}. Our experiments are currently being double-checked.

Astrophysical implications

→ The amorphous silica seems to affect the desorption kinetics of the submono- and multi- layers adsorbed onto, and therefore should be preferred to metal substrate for ISM relevant studies.

By considering fractional desorption orders for multilayers and a distribution of binding energies for sub-monolayers, we find higher *E*_{des} than generally accepted for the desorption of CO, N₂ and O₂.

→ A modification of the desorption kinetic parameters in the models could explain the discrepancy between calculated and measured gas-phase concentrations in the ISM.

→ The underestimation of the desorption energies could have led to an underestimation of the solid oxygen and nitrogen abundances. Then, a proportion of the missing oxygen could be present in the solid phase at the surface of bare and ice-coated silica in diffuse and dense clouds.

→ The thermal desorption of molecular beam-dosed O₂ from compact and porous ASW has also been investigated; the sub-monolayers desorb following 1st order kinetics with a range of binding energies. On p-ASW, O₂ is trapped within the ice pores leading to the volcano desorption of O₂ during the crystallisation of cASW (as previously observed for CO)¹³.

Temperature-Programmed Desorption gives access to the desorption rate (variation of the surface concentration *N* with time) of an adsorbate as function of the surface temperature (*T*) according to the Polanyi-Wigner equation:

$$-\frac{dN}{dt} = \nu N(t)^n \exp\left[-\frac{E_{des}}{k_B T}\right]$$

Analysis of the TPD profiles gives access to the desorption order (*n*), energy (*E*_{des}) and to the pre-exponential factor (*v*).

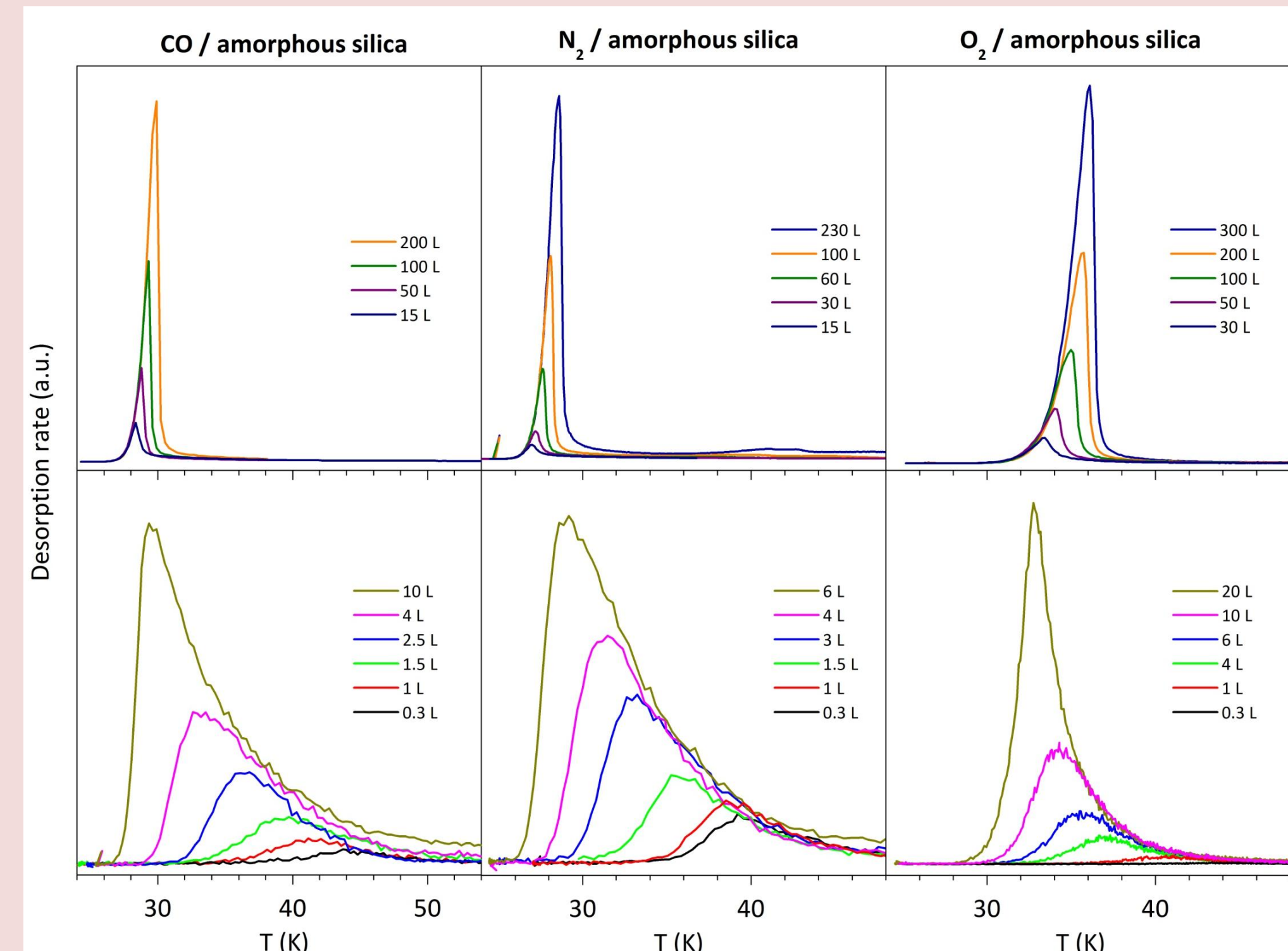


Figure 2: From left to right, TPD profiles of CO, N₂ and O₂ desorbing from the bare silica surface. The data are separated into sub-monolayer (bottom) and multilayer (top) coverages.

The TPD profiles of CO, N₂ and O₂ from amorphous silica exhibit different behaviours with coverage:

→ At low coverages (lower panel of **Fig. 2**), coincident trailing edges usually characteristic of second order recombinative desorption;

→ At intermediate coverages, both coincident leading and trailing edges: formation of 3D islands, likely to follow variable fractional desorption order, therefore not analysed in this study;

→ At high coverages (upper panel of **Fig. 2**), coincident leading edges characteristic of the zero order desorption of the multilayer.

Sub-monolayers

Coincident trailing edges on the TPD profiles (open circles on **Fig. 5(left)**) for O₂, which is usually characteristic of 2nd order desorption. This kind of desorption is not expected to occur on silica at low temperature. Instead, the porous and amorphous nature of the silica surface offers a variety of binding sites for adsorbates to bind to, with the strongest sites filled first.¹²

Direct inversion of the Polanyi-Wigner equation gives access to the *E*_{des} distribution as function of the surface concentration (**Fig. 5(right)** for O₂). A Fortran program was used to fit the TPD profiles of the sub-monolayer coverages with a range of desorption energies (assuming *v* = 10¹² s⁻¹ for 1st order desorption). The fits are presented on **Fig. 5(left)** (full lines) for O₂; the desorption energies obtained for the 3 species are displayed in **Table 2**.

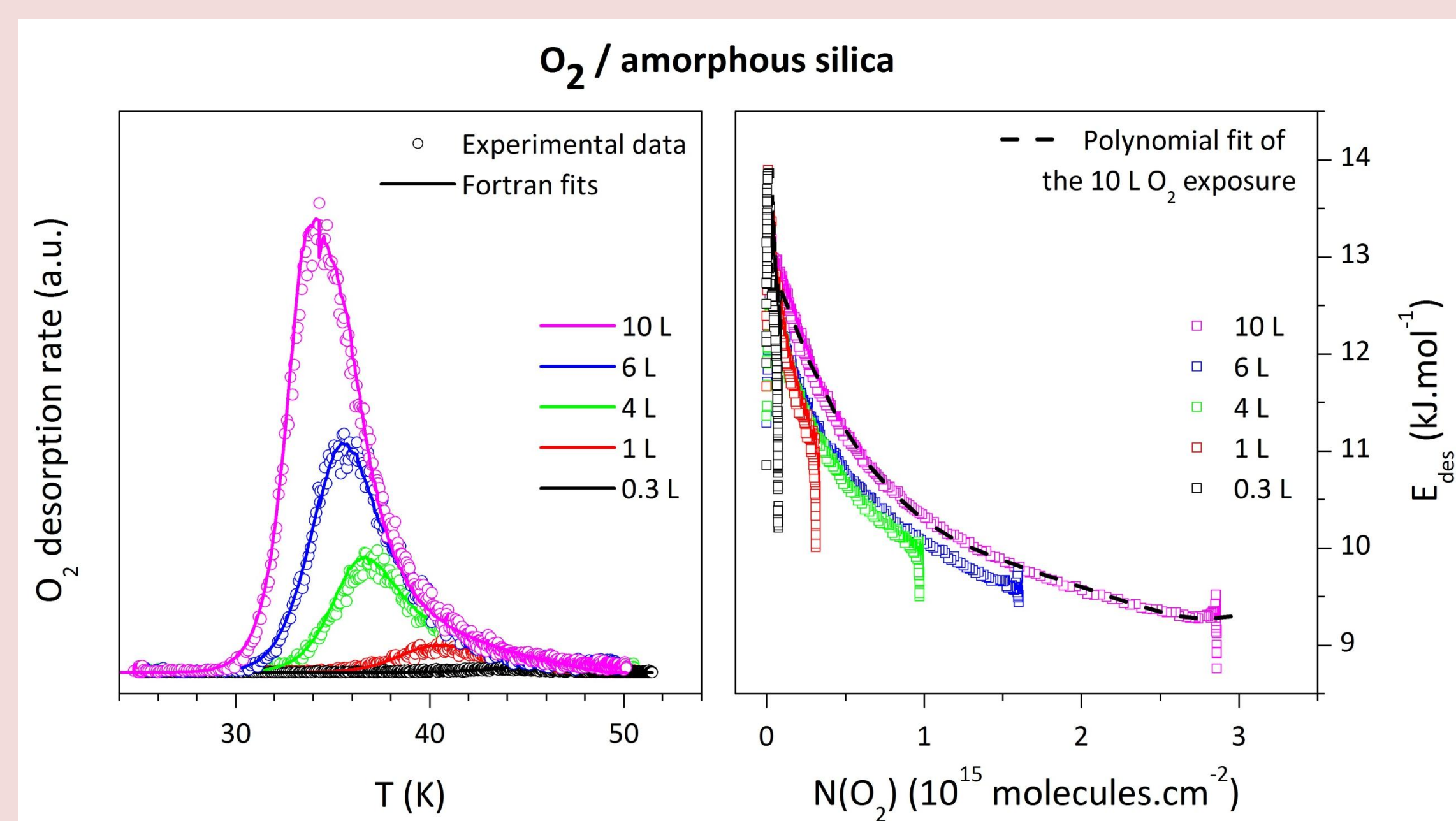


Figure 5: Left, TPD profiles (open circles) and fits (full lines) of the O₂ sub-monolayer. Right, desorption energies as function of the surface coverage.

Background dose (L)	<i>E</i> _{des} (K)		
	CO / silica	N ₂ / silica	O ₂ / silica
0.3	1419 – 1600	1551 – 1744	1455 – 1560
1	1359 – 1576	1479 – 1636	1371 – 1539
4	1131 – 1440	1200 – 1491	1227 – 1491
6	-	-	1155 – 1491
10	-	-	1119 – 1551

Table 2: Desorption energy of various sub-monolayer coverages of CO, N₂ and O₂ from bare silica.

References:

- Meyer D.M. *et al.*, ApJ, 1998, **493**, 222
- Larsson B. *et al.*, A&A, 2007, **466**, 999
- Goldsmith *et al.*, ApJ, 2000, **539**, L123
- Liseau R. *et al.*, A&A, 2012, in press
- Sandqvist Aa. *et al.*, A&A, 2008, **482**, 849
- Pontoppidan K.M. *et al.*, A&A, 2004, **426**, 225
- Hollenbach D. *et al.*, ApJ, 2009, **690**, 1497
- Chemical Kinetics Simulator (CKS), Version 1.0, IBM
- Acharyya K. *et al.*, A&A, 2007, **466**, 1005
- Fuchs G.W. *et al.*, Faraday Discussion, 2006, **133**, 331
- Noble J.A. *et al.*, MNRAS, 2012, **421**, 768
- Thrower J.D. *et al.*, MNRAS, 2009, **394**, 1510
- Collings M.P. *et al.*, 2003, ApJ, **583**, 1058

Funded by:

EPSRC

Engineering and Physical Sciences
Research Council